Abdelwahed et al. *Boundary Value Problems* (2019) 2019:23
https://doi.org/10.1186/s13661-019-1138-8

Boundary Value Problems
a SpringerOpen Journal

RESEARCH **Open Access**

Topological sensitivity analysis of a time-dependent nonlinear problem

Mohamed Abdelwahed[1*], Azhar Al Salem[1], Nejmeddine Chorfi[1] and Maatoug Hassine[2]

*Correspondence: mabdelwahed@ksu.edu.sa
[1]Department of Mathematics, College of Sciences, King Saud University, Riyadh, Saudi Arabia
Full list of author information is available at the end of the article

Abstract

We are interested in the optimization of the pipe shape allowing minimization of the dissipated energy in time-dependent Navier–Stokes Darcy flow. The used technique is based on the topological gradient method. In the theoretical part, we present an analysis of the topological sensitivity for the dissipated energy function. Some numerical tests are presented to illustrate the developed approach.

Keywords: Shape optimization; Topological sensitivity; Calculus of variations; Time-dependent Navier–Stokes equation; Darcy equation

1 Introduction

Let O be a bounded cavity of $\mathbb{R}^2$ occupied by a viscous and incompressible fluid modeled by the time-dependent nonlinear Navier–Stokes equations. We assume that the cavity O has some inlets Γ_i^k, $k = 1,\dots,n$, and some outlets Γ_o^i, $i = 1, m$ (see Fig. 1).

The aim of this work is to obtain the optimal pipes form connecting the inputs and the outputs of the cavity that minimizes the dissipated energy in the fluid under a volume constraint.

Let $S_{\text{ad}} = \{D \subset O \text{ with } \Gamma_i^k \subset \partial D \cap \partial O \text{ and } \Gamma_o^i \subset \partial D \cap \partial O \text{ with } |D| \leq V_d\}$ the set of admissible domains, where $|\cdot|$ is the measure of Lebesgue and V_d is the desired volume. For each $O \in S_{\text{ad}}$, we denote by v and p, respectively, the velocity and the pressure, solution to the Navier–Stokes equations in O

$$\begin{cases} \frac{\partial v}{\partial t} - \nu\Delta v + (v.\nabla)v + \nabla p = f & \text{in } O \times (0,T), \\ \operatorname{div} v = 0 & \text{in } O \times (0,T), \\ v = v_d & \text{on } \partial O \times (0,T). \end{cases} \tag{1}$$

ν is the fluid kinematic viscosity, T is the flow time and v_d is the boundary condition given by

$$u_d = \begin{cases} v_i^k & \text{on } \Gamma_i^l, l = 1,\dots,n, \\ v_o^i & \text{on } \Gamma_o^k, k = 1,\dots,m, \\ 0 & \text{on } \partial O \setminus \Gamma_i^l \cup \Gamma_o^k. \end{cases}$$

Figure 1 The domain O

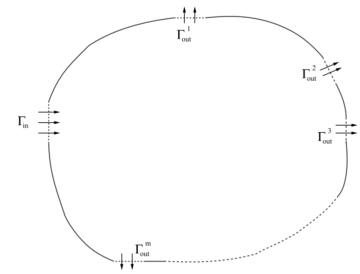

A variety of publications were focused on the design of an optimal pipe shape domain [1–3], but the majority of studies were focused on determining the optimal form of an existing boundary. The topological gradient method has been lately introduced in optimal shape problems [4–6]. This method allows for the introduction of new boundaries into the design.

The idea of the method is to measure the effect of a small topology change in the domain with respect to a given cost function. This effect is described through an asymptotic expansion of this function.

An approach using the analysis of the topological sensitivity [7–9] is presented in this work. The optimal pipe shape domain is obtained by the inserted obstacles in the initial domain. Taking into account the friction between the fluid and obstacles, which is modeled by

$$f = -\kappa(x)v(x)$$

with $\kappa(x)$ the inverse of the medium permeability [10, 11], we obtain the coupled Navier–Stokes Darcy equations

$$\begin{cases} \frac{\partial v}{\partial t} - \nu\Delta v + (v.\nabla)v + \kappa v + \nabla p = 0 & \text{in } O \times (0,T), \\ \operatorname{div} v = 0 & \text{in } O \times (0,T), \\ v = v_d & \text{on } \partial O \times (0,T). \end{cases} \tag{2}$$

The studied optimization problem is to find

$$\min_{O \in S_{\mathrm{ad}}} J_T(v),$$

where

$$J_T(v) = \int_0^T J(v)\,dt.$$

$J(v) = \nu \int_O |\nabla v|^2\,dx + \kappa \int_O |v|^2\,dx$ is the dissipation energy function and v is solution of (2).

To optimize the obstacles' location, we developed in Sect. 2 a topological asymptotic expansion of the dissipation energy function relative to the introduction of an obstacle of small size within the domain O of the fluid flow. Section 3 is devoted to the numerical tests.

2 Topological asymptotic development

Let $y \in O$, $\eta > 0$ and $\xi \subset \mathbb{R}^2$ a bounded given domain which contains the origin and $\partial\xi \in \mathcal{C}^1$. We denote $\xi_{y,\eta} = y + \eta\xi \in O$.

When an obstacle $\xi_{y,\eta}$ is inserted in O, (v_η, p_η) is solution of

$$\begin{aligned} &\frac{\partial v_\eta}{\partial t} - \nu\Delta v_\eta + (v_\eta.\nabla)v_\eta + \kappa_\eta v_\eta + \nabla p_\eta = 0 \quad \text{in } O \times (0,T), \\ &\operatorname{div} v_\eta = 0 \quad \text{in } O \times (0,T), \\ &v_\eta = v_d \quad \text{on } \partial O \times (0,T). \end{aligned} \tag{3}$$

We define the dissipation energy function associated to the perturbed domain

$$J_\eta(v_\eta) = \nu \int_{O_\eta} |\nabla v_\eta|^2\,dx + \kappa_\eta \int_{O_\eta} |v_\eta|^2\,dx,$$

where $\kappa_\eta = c_\eta \kappa$ is the perturbed impermeability with

$$c_\eta(x) = \begin{cases} c & \text{if } x \in \xi_{y,\eta}, \\ 1 & \text{if } x \in O \setminus \overline{\xi_{y,\eta}}, \end{cases}$$

and c is a contrast parameter which permits one to switch the impermeability value [12].

The variational formulation of (3) is: Find $v_\eta \in V$ solution of

$$a_\eta(v_\eta, w) = 0 \quad \forall w \in V^0, \tag{4}$$

where

$$V = \{w \in H^1(O)^d, \operatorname{div} w = 0 \text{ in } O\}, \qquad V^0 = V \cap H^1_0(O)$$

and

$$a_\eta(v, w) = \nu \int_O \nabla v.\nabla w\,dx + \int_O (v.\nabla)v.w\,dx + \int_O \kappa_\eta v.w\,dx \quad \forall v \in V.$$

In the case where $\eta = 0$, $v_\eta = v_0$ is solution of problem (1) with $\kappa_0 = \kappa$ (see [13]).

The topological gradient method consists in finding the asymptotic expansion of the cost function J with respect to a small perturbation of the initial domain. For this reason, we interested in calculate the difference between the perturbed cost function $J_\eta(u_\eta)$ and the unperturbed one $J(u_0)$. A similar study is presented in [14] for the three dimensional non-stationary Navier–Stokes equations using a numerical approximation based on the sensitivity analysis of the Stokes equation. In this work we interested in the non-stationary Navier–Stokes Darcy equations.

The variation of the studied cost function is written

$$J_\eta(u_\eta) - J(u_0) = \nu \int_O \left(|\nabla v_\eta|^2 - |\nabla v_0|^2\right) dx + \int_O \left(\kappa_\eta |v_\eta|^2 - \kappa |v_0|^2\right) dx. \tag{5}$$

In the following $|v|^2$ will be denoted by v^2 for simplification.

By remarking that

$$\begin{aligned}|\nabla v_\eta|^2 - |\nabla v_0|^2 &= 2\nabla v_0.\nabla(v_\eta - v) - 2\nabla v_0.\nabla v_\eta + (\nabla v_0)^2 + \nabla(v_\eta)^2 \\ &= 2\nabla v_0.\nabla(v_\eta - v) + (\nabla v_\eta - \nabla v_0)^2 \end{aligned} \tag{6}$$

and

$$\begin{aligned}\kappa_\eta|v_\eta|^2 - \kappa|v_0|^2 &= \kappa_\eta\big(v_\eta^2 - 2v_\eta v_0 + v_0^2\big) + 2\kappa_\eta v_\eta v_0 - \kappa_\eta v_0^2 - \kappa v_0^2 \\ &= \kappa_\eta(v_\eta - v_0)^2 + 2\kappa c_\eta v_0(v_\eta - v_0) + (c_\eta - 1)\kappa v_0^2. \end{aligned} \tag{7}$$

Following the definition of the parameter c,

$$\begin{aligned}\int_O \kappa c_\eta v_0(v_\eta - v_0)\,dx &= \int_{O\setminus\overline{\xi_{y,\eta}}} \kappa v_0(v_\eta - v_0)\,dx + \int_{\xi_{y,\eta}} \kappa v_0(v_\eta - v_0)\,dx \\ &= \int_O \kappa v_0(v_\eta - v_0)\,dx - \int_{\xi_{y,\eta}} (1-c)\kappa v_0(v_\eta - v_0)\,dx. \end{aligned} \tag{8}$$

Using (6)–(8), we get

$$\begin{aligned}J_\eta(u_\eta) - J(u_0) = {}& 2\nu\int_O \nabla v_0.\nabla(v_\eta - v_0)\,dx + \nu\int_O (\nabla v_\eta - \nabla v_0)^2\,dx \\ &+ \int_O \kappa_\eta|v_\eta - v_0|^2\,dx + 2\int_O \kappa v(v_\eta - v_0)\,dx \\ &- 2\int_{\xi_{y,\eta}} (1-c)\kappa v_0(v_\eta - u_0)\,dx - \int_{\xi_{y,\eta}} (1-c)\kappa|v_0|^2\,dx. \end{aligned} \tag{9}$$

By using (4) and the integration by parts

$$\begin{aligned}&\nu\int_O \nabla(v_\eta - v_0).\nabla w\,dx + \int_O \big((v_\eta.\nabla)v_\eta - (v_0.\nabla)v_0\big).w\,dx + \int_O (\kappa_\eta v_\eta - \kappa v_0).w\,dx \\ &\quad = \nu\int_O \nabla(v_\eta - v_0).\nabla w\,dx + \int_O \big((v_0.\nabla)w + (\nabla w)v_0\big).(v_\eta - v_0)\,dx \\ &\qquad + \int_O \big(\nabla(v_\eta - v_0)\big)(v_\eta - v_0).w\,dx + \int_O \kappa(v_\eta - v_0).w - \int_{\xi_{y,\eta}} (1-c)\kappa v_\eta.w\,dx \\ &\quad = 0. \end{aligned} \tag{10}$$

By choosing $w = v_{\mathrm{adj}}$, the solution of the adjoint problem associated to (2), we obtain

$$\begin{aligned}&\nu\int_O \nabla(v_\eta - v_0).\nabla v_{\mathrm{adj}}\,dx + \int_O \big((v.\nabla)v_{\mathrm{adj}} + (\nabla v_{\mathrm{adj}})v\big).(v_\eta - v)\,dx \\ &\qquad + \int_O \kappa(v_\eta - v).v_{\mathrm{adj}}\,dx \\ &\quad = (1-c)\int_{\xi_{y,\eta}} \kappa v_\eta.v_{\mathrm{adj}}\,dx - \int_O \big(\nabla(v_\eta - v_0)\big)(v_\eta - v_0).v_{\mathrm{adj}}\,dx. \end{aligned} \tag{11}$$

Using the variational formulation of the divergence free adjoint equation (see [15, 16]) and choosing $w = v_\eta - v_0$, we obtain

$$\begin{aligned}&\nu \int_O \nabla v_{\mathrm{adj}}.\nabla(v_\eta - v_0) + \int_O \bigl((v.\nabla)v_{\mathrm{adj}} + (\nabla v_{\mathrm{adj}})v\bigr).(v_\eta - v_0)\,dx\\&\quad + \int_O \kappa v_{\mathrm{adj}}.(v_\eta - v_0)\,dx\\&\quad = 2\nu \int_O \nabla v.\nabla(v_\eta - v_0)\,dx + 2\int_O \kappa v.(v_\eta - v_0)\,dx.\end{aligned} \tag{12}$$

By comparing this last equation with (11), we obtain

$$\begin{aligned}&2\nu \int_O \nabla v.\nabla(v_\eta - v_0)\,dx + 2\int_O \kappa v.(v_\eta - v_0)\,dx\\&\quad = (1-c)\int_{\xi_{y,\eta}} \kappa v_\eta.v_{\mathrm{adj}}\,dx - \int_O \bigl(\nabla(v_\eta - v_0)\bigr)(v_\eta - v_0).v_{\mathrm{adj}}\,dx.\end{aligned} \tag{13}$$

By substituting (13) in (9), we obtain

$$\begin{aligned}J_\eta(v_\eta) - J(v_0) &= (1-c)\int_{\xi_{y,\eta}} \kappa v_\eta.v_{\mathrm{adj}}\,dx - \int_{\xi_{y,\eta}} (1-c)\kappa|v_0|^2\,dx\\&\quad - \int_O \bigl(\nabla(v_\eta - v_0)\bigr)(v_\eta - v_0).v_{\mathrm{adj}} + \nu\int_O (\nabla v_\eta - \nabla v_0)^2\,dx\\&\quad + \int_O \kappa_\eta|v_\eta - v_0|^2\,dx - 2\int_{\xi_{y,\eta}} (1-c)\kappa v(v_\eta - v_0)\,dx\\&= \Sigma(\eta) - \int_{\xi_{y,\eta}} (1-c)\kappa v_0.(v_0 - v_{\mathrm{adj}})\,dx,\end{aligned} \tag{14}$$

where

$$\begin{aligned}\Sigma(\eta) &= \int_O |\nabla v_\eta - \nabla v_0|^2\,dx + \int_O \kappa_\eta|v_\eta - v_0|^2\,dx - 2\int_{\xi_{y,\eta}} (1-c)\kappa v_0(v_\eta - v_0)\,dx\\&\quad + \int_{\xi_{y,\eta}} (1-c)\kappa v_{\mathrm{adj}}.(v_\eta - v_0)\,dx - \int_O \bigl(\nabla(v_\eta - v_0)\bigr)(v_\eta - v_0).v_{\mathrm{adj}}\,dx.\end{aligned}$$

We remark that it can be shown that $\Sigma(\eta) = O(\eta^2)$. Finally, using the Lebesgue differentiation theorem [17], we obtain

$$J_\eta(v_\eta) = J(v_0) - |\xi_{y,\eta}|(1-c)\kappa(y)v_0(y)\bigl(v_0(y) - v_{\mathrm{adj}}(y)\bigr) + \Sigma(\eta), \tag{15}$$

which gives the following result.

Theorem 2.1 *The function J satisfies the asymptotic development*

$$J_\eta(v_\eta) - J(v) = f(\eta)DJ(y) + o\bigl(f(\eta)\bigr), \tag{16}$$

where $f(\eta) = |\xi_{y,\eta}|$ and DJ is the topological gradient given by

$$DJ(y) = -(1-c)\kappa(y)v(y)\bigl(v(y) - v_{\mathrm{adj}}(y)\bigr), \quad \forall y \in O. \tag{17}$$

Corollary 2.1 *Summing over time, the topological gradient of $J_T(v)$ is given by*

$$DJ_T(v) = -(1-c)\kappa(y)\int_0^T v(y)\big(v(y) - v_{\text{adj}}(y)\big)\,dt. \tag{18}$$

3 Numerical results

3.1 Optimization algorithm

Using (16), we remark that $J_\eta(v_\eta) < J(v)$ if $DJ(y) < 0$. Then the minimum of J, which corresponds to the best location y of the obstacle, is obtained where $DJ(y)$ is the most negative.

Following this result, we propose the following numerical algorithm: We begin first by choosing $O_0 = O$. Then we construct the sequence of domains $(O_k)_{k\geq 0}$ such that $O_{k+1} = O_k \setminus \overline{\xi_k}$, where ξ_k is the obstacle defined by a level set curve of $D_k J_T$

$$\xi_k = \big\{x \in \Omega_k, \text{such that } 0 \geq d_k \geq D_k J_T(x)\big\}.$$

Here, d_k is a given constant and $D_k J_T(y) = DJ_T(v^k)$ is defined by

$$DJ_T\big(v^k\big) = -(1-c)\kappa(y)\int_0^T v^k(y)\big(v^k(y) - v^k_{\text{adj}}(y)\big)\,dt. \tag{19}$$

v^k is the solution of the Navier–Stokes Darcy problem

$$\begin{cases} \frac{\partial v^k}{\partial t} - \nu\Delta v^k + (v^k.\nabla)v^k + \kappa v^k + \nabla p^k = 0 & \text{in } O_k \times (0,T),\\ \operatorname{div} v^k = 0 & \text{in } O_k \times (0,T),\\ v^k = v_d & \text{on } \partial O \times (0,T). \end{cases} \tag{20}$$

v^k_{adj} is the solution to the adjoint problem of (20), given by (see [15])

$$\begin{cases} -\frac{\partial v^k_{\text{adj}}}{\partial t} - \nu\Delta v^k_{\text{adj}} - \nabla v^k_{\text{adj}}.v^k - (v^k.\nabla)v^k_{\text{adj}} & \\ \quad + \kappa v^k_{\text{adj}} + \nabla p^k_{\text{adj}} = \frac{\partial J}{\partial v^k} & \text{in } O_k \times (0,T),\\ -\operatorname{div} v^k_{\text{adj}} = \frac{\partial J}{\partial p^k} & \text{in } O_k \times (0,T),\\ v^k_{\text{adj}}(T) = 0 & \text{in } O_k,\\ (v^k_{\text{adj}})_t = 0 & \text{on } \partial O \times (0,T),\\ (v^k_{\text{adj}})_n = \frac{\partial J_{\partial O}}{\partial p} & \text{on } \partial O \times (0,T), \end{cases} \tag{21}$$

where $(v^k_{\text{adj}})_t$ and $(v^k_{\text{adj}})_n$ are, respectively, the tangential and normal component of v^k_{adj} and $J_{\partial O}$ is the boundary part of J.

3.2 Numerical discretization

The numerical resolution of the Navier–Stokes Darcy problem (20) and its adjoint problem is done on two steps. To overcome the problem of nonlinearity terms in the first equation, we use the characteristics method [18]. It consists of approximating the convection term as

$$\left(\frac{\partial v^k}{\partial t} + \big(v^k.\nabla\big)v^k\right)\big(x,t^{n+1}\big) = \frac{1}{\Delta t}\big(v^k\big(x,t^{n+1}\big) - v^k\big(X\big(x,t^{n+1},t^n\big),t^n\big),$$

where Δt is the time step, $t^n = n\Delta t$ and $X(x, t^{n+1}, t^n)$ is the position at time t^n of the fluid particle which is located at x at time t^{n+1}.

The time discretization of problem (20) can then be written

$$\begin{cases} \lambda v_{n+1}^k - \nu\Delta v_{n+1}^k + \nabla p_{n+1}^k = g_n & \text{in } O_k, \\ \operatorname{div} v_{n+1}^k = 0 & \text{in } O_k, \\ v_{n+1}^k = v_d & \text{on } \partial O, \end{cases} \tag{22}$$

where $\lambda = \frac{1}{\Delta t} + \kappa$, $g_n = \frac{1}{\Delta t} v^k(X(x, t^{n+1}, t^n), t^n)$, $v_{n+1}^k = v^k(\cdot, t^{n+1})$.

It is shown that the weak formulation of obtained discrete problem (22) has a unique solution [19].

In the same way, we can express the objective function by

$$DJ_T(v^k) = -(1-c)\kappa \sum_{n=0}^{N} v_n^k \left(v_n^k - \left(v_{\text{adj}}^k\right)_n\right),$$

where v_n^k and $(v_{\text{adj}}^k)_n$ are, respectively, the numerical solution of the Navier–Stokes Darcy problem and its adjoint at time t^n.

For the spatial discretization of problems (22) and the time discrete adjoint problem (21), We use the finite element method.

3.3 Example 1

In this test, the domain O is taken as the square with side equal to 1 containing one input Γ_i and one output Γ_o. A Dirichlet parabolic profile is, respectively, prescribed at Γ_i and Γ_o with maximum inflow and outflow equal to 1. On the other part of the boundary $\partial O_k \setminus (\Gamma_i \cup \Gamma_o)$ a homogeneous Dirichlet condition is imposed.

d_k is selected in practice such that $J_T(O_{k+1}) - J_T(O_k)$ is negative. It determines the obstacle volume. In numerical tests, we choose d_k such that $\xi_k \subset O_k$, $DJ_T \leq 0$ and $|\xi_k| \leq 0.1|O_k|$.

As the optimal design of the pipe depends on the position of the input and the output, we consider two different cases (a) (see Fig. 2) and (b) (see Fig. 3) with different input and output positions.

We use the presented algorithm in order to find the pipe optimal domain connecting the inlet of the cavity and its outlet with minimum dissipated energy.

We present, in Figs. 4 and 5 (respectively, Figs. 6 and 7) two intermediate geometries obtained throughout the optimization process for the case (a) (respectively, the case (b)).

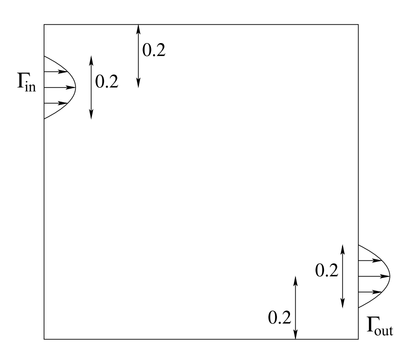

Figure 2 Pipe bend initial domain: Case (a)

Figure 3 Pipe bend initial domain: Case (b)

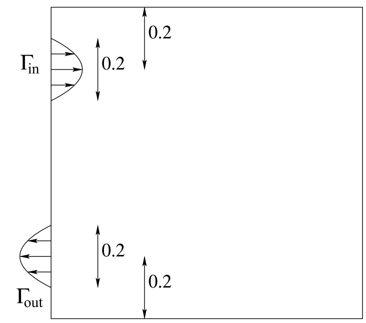

Figure 4 Case (a): Intermediate domain

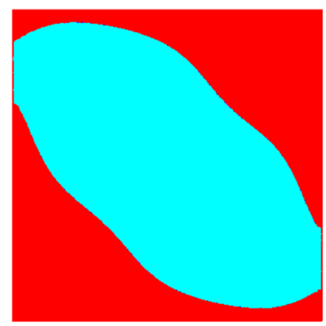

Figure 5 Case (a): Intermediate domain

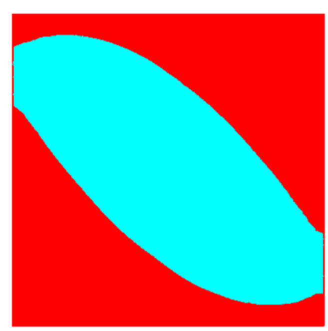

Figure 6 Case (b): Intermediate domain

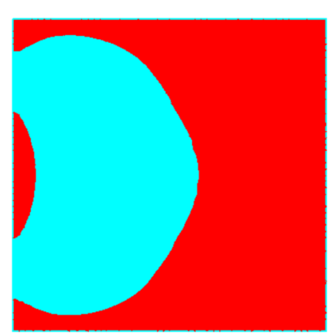

The obtained optimal domain is presented for the case (a) (respectively, the case (b)) in Fig. 8 (respectively, Fig. 9). It corresponds to $V_d = 0.1\pi|\Omega|$ (respectively, $V_d = 0.08\pi|\Omega|$).

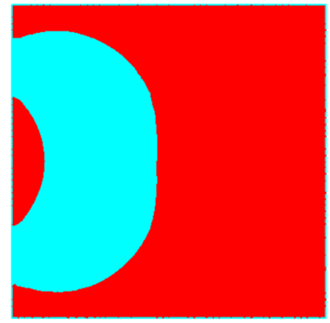

Figure 7 Case (b): Intermediate domain

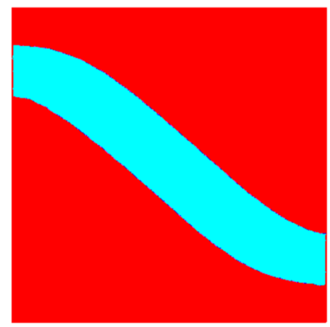

Figure 8 Case (a): Optimal pipe domain

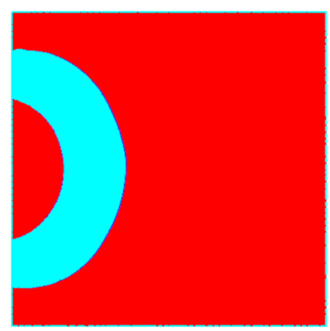

Figure 9 Case (b): Optimal pipe domain

3.4 Example 2

In this example, $\Omega =]0, 3/2[\times]0, 1[$ is a rectangular domain with two inlets and outlets, The considered boundary condition is similar to that considered for the pipe example. As in the previous example, we consider here two cases describing various relative positions of inlets and outlets. The domains of the considered cases, showing inlets and outlets positions, are depicted in Figs. 10 (Case (c)) and 11 (Case (d)).

The geometries obtained during the optimization process are presented respectively in Figs. 12–13 for the case (c) and Figs. 14–15 for the case (d). The optimal geometries plotted in Figs. 16 and 17 are respectively computed with $V_d = \frac{1}{5}|\Omega|$ for the case (c) and $V_d = \frac{1}{6}|\Omega|$ for the case (d).

4 Conclusion

We developed in this work an efficient topological optimization algorithm for determining the optimal shape design of unsteady flow described by the coupled Navier–Stokes and

Figure 10 Double pipe initial domain: Case (c)

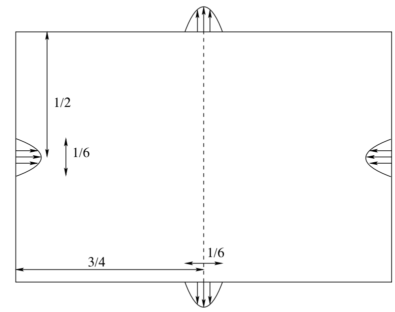

Figure 11 Double pipe initial domain: Case (d)

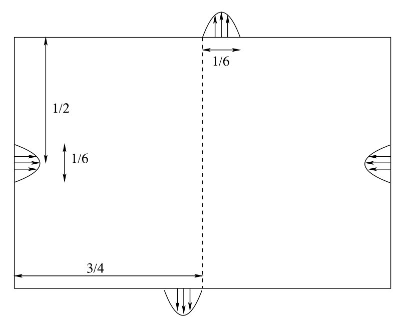

Figure 12 Case (c): Intermediate domain

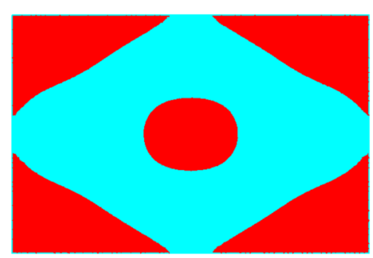

Figure 13 Case (c): Intermediate domain

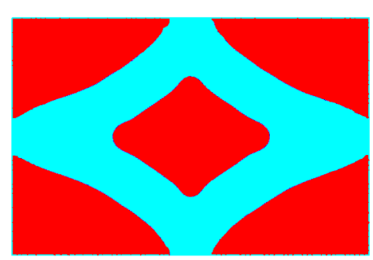

Darcy equations. Using the asymptotic expansion of the energy function, the obtained optimal domain is generated by inserting obstacles at each iteration until reaching the desired volume. The location of these obstacles is determined by the developed topological gradient. This problem can be generalized to the three dimensional case and used for realistic applications such the bypass problem in biomedical fluid.

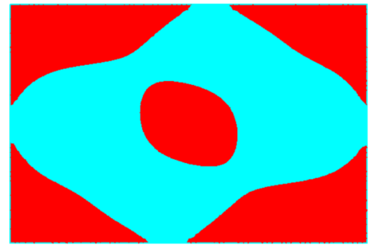

Figure 14 Case (d): Intermediate domain

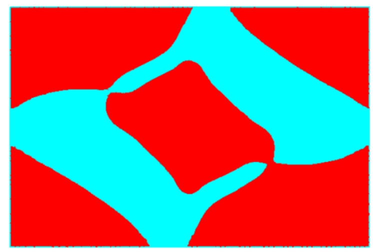

Figure 15 Case (d): Intermediate domain

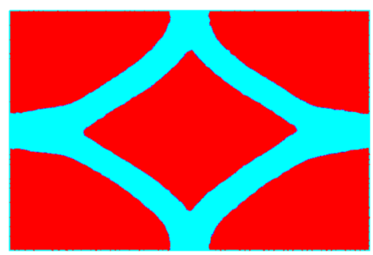

Figure 16 Case (c): Optimal double pipe domain

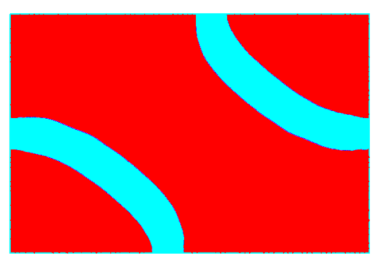

Figure 17 Case (d): Optimal double pipe domain

Acknowledgements
The authors would like to extend their sincere appreciation to the Deanship of Scientific Research at King Saud University for funding this Research group No. (RG-1435-026).

Funding
Not applicable.

Availability of data and materials
Not applicable.

Competing interests
The authors declare that they have no competing interests.

Authors' contributions
The authors declare that the study was realized in collaboration with equal responsibility. All authors read and approved the final manuscript.

Author details
[1]Department of Mathematics, College of Sciences, King Saud University, Riyadh, Saudi Arabia. [2]Department of Mathematics, Monastir University, Monastir, Tunisia.

Publisher's Note

Springer Nature remains neutral with regard to jurisdictional claims in published maps and institutional affiliations.

Received: 6 January 2019 Accepted: 20 January 2019 Published online: 30 January 2019

References

1. Afshar, M.H., Afshar, A., Marino, M.A., Asce, H.M.: An iterative penalty method for the optimal design of pipe networks. Int. J. Civ. Eng. **7**(2), 1–16 (2009)
2. Pingen, G.: Optimal design for fluidic systems: topology and shape optimization with the lattice Boltzmann method. Ph.D. thesis, University of Colorado (2008)
3. Mohammadi, B., Pironneau, O.: Applied Shape Optimization for Fluids. Oxford University Press, New York (2001)
4. Abdelwahed, M., Hassine, M.: Topological optimization method for a geometric control problem in Stokes flow. Appl. Numer. Math. **59**(8), 1823–1838 (2009)
5. Borrvall, T., Petersson, J.: Topological optimization of fluids in Stokes flow. Int. J. Numer. Methods Fluids **44**(1), 77–107 (2003)
6. Guest, J.K., Prévost, J.H.: Topology optimization of creeping fluid flows using a Darcy–Stokes finite element. Int. J. Numer. Methods Eng. **66**, 461–484 (2006)
7. Guillaume, P., Sid Idris, K.: Topological sensitivity and shape optimization for the Stokes equations. SIAM J. Control Optim. **43**(1), 1–31 (2004)
8. Hassine, M., Masmoudi, M.: The topological asymptotic expansion for the quasi-Stokes problem. ESAIM Control Optim. Calc. Var. **10**(4), 478–504 (2004)
9. Sokolowski, J., Zochowski, A.: On the topological derivative in shape optimization. SIAM J. Control Optim. **37**(4), 1251–1272 (1999)
10. Gersborg-Hansen, A., Sigmund, O., Haber, R.B.: Topology optimization of channel flow problems. Struct. Multidiscip. Optim. **30**(3), 181–192 (2005)
11. Yongbo, D.: Topology optimization of steady and unsteady incompressible Navier–Stokes flows driven by body forces. Struct. Multidiscip. Optim. **47**(4), 555–570 (2013)
12. Gartling, D.K., Hickox, C.E., Givler, R.C.: Simulation of coupled viscous and porous flow problems. Comput. Fluid Dyn. J. **7**(1), 23–48 (1996)
13. Rădulescu, V., Repovš, D.: Partial Differential Equations with Variable Exponents: Variational Methods and Qualitative Analysis. Taylor & Francis, Boca Raton (2015)
14. Abdelwahed, M., Hassine, M.: Topology optimization of time dependent viscous incompressible flows. Abstr. Appl. Anal. **2014**, Article ID 923016 (2014)
15. Hasund, K.E.: Toplogy optimization for unsteady flow with applications in biomedical flows. Ph.D. thesis, Norwegian University of Sciences and Technology (2017)
16. Rădulescu, V.: Nonlinear elliptic equations with variable exponent: old and new. Nonlinear Anal., Theory Methods Appl. **121**, 336–369 (2015)
17. Rudin, W.: Real and Complex Analysis. Mathematics Series. McGraw-Hill, New York (1987)
18. Pironneau, O.: On the transport diffusion algorithm and its applications to Navier–Stokes equations. Numer. Math. **38**, 309–332 (1982)
19. Brezzi, F., Fortin, M.: Mixed and Hybrid Finite Element Methods. Springer, New York (1991)